Proceedings of the Institute of Acoustics

INFLUENCE OF GROUND ROUGHNESS ON OUTDOOR SOUND

K Attenborough

Faculty of Technology, The Open University, Walton Hall, Milton Keynes, MK7 6AA

1. INTRODUCTION

Considerable effort has been devoted to the effects of the finite impedance of the ground surface on sound propagation outdoors[1]. Less attention has been paid to the possible influences of the roughness of the ground, where the mean roughness height is small compared with a wavelength even though the effects of such surface roughness have been and are being studied intensively by the underwater acoustics community[2-4]. In particular the existence of the predicted rough surface boundary wave has been verified experimentally by pulse experiments[5-7].
Tolstoy[2] has distinguished between two theoretical approaches, for predicting the *coherent* field resulting from co-operative forward scatter by boundary roughnesses where the typical roughness height and spacing is small compared to a wavelength. Both of these reduce the rough surface scattering problem to one that uses a suitable boundary condition at a *smoothed* boundary. According to Tolstoy[2] the *boss* method, originally derived by Biot[8] and Twersky[9], has the advantages that (i) it is more accurate to first order than *perturbation* methods (ii) it may be used even in conditions where the roughness shapes introduce steep slopes and (iii) it is reasonably accurate even when the roughness size approaches a wavelength. Tolstoy and others have
predicted the possibility that ground roughness enables penetration of underwater sound into the shadow zone formed by an upward refraction[10,11]. Howe[12] has considered propagation over a rough finite impedance boundary. Howe laid stress on the prediction of an enhanced surface wave component in the context of long range sound propagation at low frequencies and grazing-incidence over hilly terrain with relatively acoustically-hard surfaces.
An important conclusion of previous work is that the *normal surface impedance or admittance of the boundary is modified by the coherent forward scatter associated with the presence of roughness.* The surface admittance is known to have an influence on the attenuation spectrum due to destructive and constructive interference between direct and ground-reflected sound paths from a point source after allowing for wavefront spreading and atmospheric absorption. This excess attenuation spectrum is known as *ground effect* and is an important factor in studies of outdoor sound, particularly from continuous sources at near-grazing incidence[1].
A reconciliation, combination and extension of Howe's and Tolstoy's results[8,4], enables predictions of finite impedance ground effect (in the form of excess attenuation spectra) for elevated point source and receiver in the presence of ground surfaces with arbitrary roughness shapes and concentrations, and these predictions have been validated by laboratory measurements[13]. In this paper the results of Howe's and Tolstoy's analyses of propagation over acoustically-hard and soft rough boundaries are given and Tolstoy's analysis of propagation into the underwater shadow zone[10] is repeated for the *atmospheric* upward refraction case. Far-field predictions are made for realistic impedances and roughnesses after taking into account incoherent scatter[14].

2. EFFECTIVE ADMITTANCE THEORY

Propagation over a rough rigid-porous boundary where the roughnesses and their spacing are small compared with a wavelength may be predicted from adaptation of the Biot/Tolstoy/Lighthill[3] theory for propagation at a rough fluid interface. The rigid-porous lower medium and the (rigid-porous) roughness may be modelled as effective fluids with complex densities and sound speeds.

The theory requires that $k_o h < k_o \ell \lesssim 1$, where k_0 is the wave number in the upper half-space h is the mean roughness height and ℓ is the mean centre-to-centre spacing of the roughnesses.

A general (two-sided) boundary condition for the perturbed field potential in the half space ($\rho_1 c_1$) above the boundary of a fluid (ρ_3,c_3) containing three-dimensional fluid roughnesses (ρ_2,c_2) is given by[3]

$$\frac{\partial \phi_1}{\partial z} - \frac{\partial \phi_3}{\partial z} = ik_o \beta_3 * \phi_1 + \varepsilon_{12} \delta_{12} \frac{\partial^2 \phi_1}{\partial z^2} \qquad (1)$$

where ϕ_1 is the perturbed field potential in the upper half-space, ϕ_3 is that in the lower half-space, time dependence exp ($i\omega t$) is understood and the effective relative admittance of the rough surface, β_3^*, is given by

$$\beta_3^* = ik_o \varepsilon + \beta \qquad (2)$$

$$\varepsilon = \varepsilon_{12} + \left(\frac{\rho_1 c_1^2}{\rho_3 c_3^2}\right) \varepsilon_{32} + \frac{\rho_1}{\rho_3}\left[1 - \frac{c_1^2}{c_3^2}\right] \varepsilon_{32} \delta_{32}$$

$$\varepsilon_{ij} = a_{ij} - b_{ij} \qquad \varepsilon_{ij} \delta_{ij} = a_{ij}$$

$$a_{ij} = 3\sigma_v \left[\frac{\rho_j - \rho_i}{\rho_i + \rho_j}\right] \frac{s_{3D}}{v_{3D}} \qquad b_{ij} = \sigma_v \left[1 - \frac{\rho_i c_i^2}{\rho_j c_j^2}\right]$$

$$s_{3D} = \left[\frac{\rho_i + 2\rho_j}{\rho_j + K\rho_i}\right] \frac{s_3}{2}$$

$$v_{3D} = 1 + \frac{3\pi\sigma_v}{8N\ell^3} \left[\frac{\rho_j - \rho_i}{\rho_j + \rho_i / 2}\right] s_{3D}$$

$\beta = \dfrac{\rho_1 c_1}{\rho_2 c_2}$ represents the relative normal admittance of the lower half space.

S_3 is a shape factor defined later.

Similarly, the effective relative admittance of a two-dimensionally-rough fluid interface is given by

$$\beta_2^* = ik_1 \cos^2\theta\, \varepsilon + \beta \qquad (3)$$

where a_{ij} is replaced by $a_{2ij} = 2\sigma_v \left[\dfrac{\rho_j - \rho_i}{\rho_j + \rho_i}\right] \dfrac{s_{2D}}{v_{2D}}$,

$$s_{2D} = \frac{\rho_i + \rho_j}{\rho_j + K\rho_i} s_2 \quad \text{and} \quad v_{2D} = 1 + \frac{2\pi\sigma_v}{3N\ell^2}\left[\frac{\rho_j - \rho_i}{\rho_v + \rho_i}\right].$$

For $\rho_2 = \rho_3$, $c_2 = c_3$, $|\rho_3| >> \rho_1$, the expressions for effective relative admittance of the rough surface may be simplified to

$$\beta_3^* \simeq \left(1 - ik_g\sigma_v\right)\beta - ik_0(\sigma_v/2)\left(3s_3/v_2 - 2\right) \tag{4}$$

$$\beta_2^* \simeq \left(1 - ik_g\sigma_v\right)\beta - ik_0\cos^2(\theta)\sigma_v\left(2s_2/v_2 - 1\right) \tag{5}$$

where k_g is the complex propagation constant in lower half-space,
Shape Factors s_3 and s_2 are given by,

$$s_3 = \frac{2}{3}(1 + K),\; s_2 = \frac{1}{2}(1 + K)$$

where $K = \dfrac{\text{entrained fluid mass}}{\text{mass of fluid displaced by scatter}}$

and $K = \frac{1}{2}$ for hemispheres, $K = 1$ for semicylinders.

Dipole interaction factors, v_3 and v_2, are given by

$$v_3 = 1 + \frac{3\pi}{8}\left(\frac{\sigma_V s_3}{N\ell^3}\right), \qquad v_2 = 1 + \frac{2\pi}{3}\left(\frac{\sigma_V s_2}{N\ell^2}\right)$$

where N = number of scatterers per unit area
Equivalent forms that may be deduced from the results of Howe[12] are

$$\beta_3^* = \left(1 + \sigma_A\right)\beta - ik_0\frac{\sigma_V}{2}\left(\frac{3s_3}{v_3} - 2\right) \tag{6}$$

$$\beta_2^* = \left[1 + \left(\frac{\pi}{2} - 1\right)\sigma_A\right]\beta - ik_0\,\sigma_V\cos^2(\theta)\left(\frac{2s_2}{v_2} - 1\right) \tag{7}$$

where σ_A represents the area of scatterers per unit area of the rough surface.
Given any of these forms for effective relative admittance, it is possible to calculate the excess attenuation (EA) above an arbitrarily rough finite impedance boundary using the classical form for propagation from a point source over an impedance boundary[1].

3. PROPAGATION IN A BILINEAR VELOCITY GRADIENT ABOVE A ROUGH IMPEDANCE SURFACE

Following Tolstoy[10], we require the solution of

$$\frac{\partial^2\phi}{\partial z^2} + \gamma^2(z)\phi = 0,\; z > 0 \tag{8}$$

where $\gamma^2(z) = k^2 - K^2$, K is horizontal wave number
$k = \omega / c(z)$

INFLUENCE OF GROUND ROUGHNESS

$$c(z) = \left(\frac{1}{c_0^2} + qz\right)^{-1/2},$$

subject to $$\frac{\partial\phi}{\partial z} = -\varepsilon\left(k_0^2 + \delta\frac{\partial^2}{\partial z^2}\right)\phi, \quad z = 0 \qquad (9),$$

where $\varepsilon = \frac{\sigma_V}{2}\left(\frac{3s}{v} - 2\right) - i\left(1 + \sigma_A\right)\frac{\beta}{k_0}$ or $\frac{\sigma_V}{2}\left(\frac{3s}{v} - 2\right) - i\left(1 + ik_g\sigma_V\right)\frac{\beta}{k_0}$

and $\delta = \frac{3\sigma_V s}{2\varepsilon v}$.

If source and receiver are on the boundary, then the solution may be written,

$$\phi = \frac{1}{2\pi}e^{i\omega t}\int_0^\infty \frac{H_{1/3}^{(2)}(S_0)}{H_{-\frac{2}{3}}^{(2)}(S_0) - \varepsilon\left(\delta - k_0^2/\gamma_0^2\right)\gamma_0 H_{\frac{1}{3}}^{(2)}(S_0)}\frac{1}{\gamma_0}J_0(Kr)KdK \qquad (10)$$

where $S_0 = \frac{2}{3p}\gamma_0^3$, $\gamma_0^2 = k_0^2 - K^2$, $p = \omega^2 q$, and $H^{(2)}$ are Hankel functions of the second kind.

Note that p may be positive or negative. However in the remainder of this contribution we concentrate on $p \geq 0$, corresponding to a homogeneous or upward refracting atmosphere. If equation (10) is rewritten in the form

$$\phi = \frac{1}{2\pi}e^{i\omega t}\int_0^\infty \frac{1}{\gamma_0\frac{H_{-2/3}^{(2)}(S_0)}{H_{1/3}^{(2)}(S_0)} - \varepsilon\left(\gamma_0^2\delta - k_0^2\right)}J_0(Kr)KdK \qquad (11)$$

then it is easier to deduce both the approximate form of solution and the relationship with standard results for special cases.

In particular it should be noted that (12) reduces to the standard integral[15] for propagation over a smooth impedance plane in the absence of a velocity gradient and roughness. The reduced form for $p > 0$, and no roughness may be seen to be related to the standard integral for this case[16] when the relationships between Hankel functions of one-or two-thirds order and Airy functions are invoked.

4. FAR-FIELD SOLUTIONS AT GRAZING-INCIDENCE

The boundary wave over a *hard rough* surface in the shadow zone, for weak gradients and high frequencies may be calculated from

$$\phi_B \simeq \frac{e^{3i\pi/4}}{\sqrt{2\pi k_0 r}}\varepsilon_1 k_0^2 e^{-\delta_B r}e^{-i(k_0 r - \omega t)} \qquad (12)$$

where $\delta_B \simeq \varepsilon_1^2 k_0^3 \exp\left(-\frac{4\varepsilon_1^3 k_0^4}{3qc_0^2}\right)$.

INFLUENCE OF GROUND ROUGHNESS

The ratio of the rough surface boundary wave to the first term of the diffracted field in the far-field[10] is given by

$$\left|\frac{\phi_B}{\phi_d}\right| \simeq 2p^{-1/3}\,\varepsilon_1 k_0^{\,2}\, X_1 \exp\left(\delta_1 - \delta_B\right) r \qquad (13)$$

where $\varepsilon_1 \simeq \frac{1}{2}$ (scatterer volume above plane per unit area).

The solution of equation (12) can, in general, be approximated by a residue series summation. Again the total field is given by a diffracted contribution plus a surface wave corresponding complex γ.

Hence $\phi = \phi_d + \phi_B$, where

the diffracted field is given by

$$\phi_d = \frac{ip}{4}\sum_m \frac{H_0^{(2)}\left(K_m r\right)e^{i\omega t}}{\gamma_{0m}^{\,2} + p\varepsilon\delta + \varepsilon^2\left(k_0^2 - \delta\gamma_{0m}^{\,2}\right)^2} \qquad (14)$$

and the roughness induced surface wave may be approximated by

$$\phi_B \simeq \frac{i\varepsilon k_0^{\,2}}{\sqrt{2\pi k_0 r}}\left[1 + \frac{0.541}{w_{0B}}\right]\exp\left(-\alpha_B r\right)\exp\left[-i\left(k_0 r - \omega t - \frac{\pi}{4}\right)\right] \qquad (15)$$

where $\alpha_B \simeq \mathrm{Re}\left[\varepsilon^2 k_0^{\,3}\, e^{-2w_{0B}}\left(1 + \frac{7}{36}\,\frac{1}{w_{0B}}\right)\right]$

and $\quad w_{0B} \simeq \left|\frac{2\varepsilon^3 k_0^{\,6}}{3p}\right|$.

γ_{0m}, $K_m \left(= \sqrt{\left(\gamma_{0m}^2 - k_0^2\right)}\right)$ are solutions of

$$\gamma_0\left[H_{-2/3}^{(2)}\left(S_0\right)/H_{1/3}^{(2)}\left(S_0\right)\right] - \varepsilon\left(\delta\gamma_0^2 - k_0^2\right) = 0 \qquad (16)$$

which requires numerical solution in general.

5. ATTENUATION OF BOUNDARY WAVE DUE TO INCOHERENT SCATTER

The presence of surface roughness leads to incoherent as well as coherent scatter. Consequently the amplitudes of the roughness-induced boundary waves are decreased. Tolstoy[14] has considered this attenuation for a general rough two-fluid interface.

Hence for a rough two-fluid interface, the attenuation constants are given by

$$\alpha_{3D} = \frac{1}{4\pi N}\,\frac{g_1\left(A^2 + \frac{1}{3}b_3^2\right)}{1 + \rho_1 g_1/\rho_2 g_2}\,k_0^{\,4} \qquad (17)$$

$$\alpha_{2D} = \frac{1}{2N}\,\frac{g_1\left(A^2 + \frac{1}{2}b_2^{\,2}\right)}{1 + \rho_1 g_1/\rho_2 g_2}\,k_0^{\,3} \qquad (18)$$

where $g_{1,2}$ are roots of the characteristic equation for the rough surface boundary wave,

$$A = \sigma_v \left(1 - \rho_1 c_1^2 / \rho_2 c_2^2\right),$$

$$b_3 = \frac{3\sigma_v s_{3D}}{2} \left(1 - \rho_1 / \rho_2\right),$$

$$b_2 = 2\sigma_v s_{2D} \left(1 - \rho_1 / \rho_2\right),$$

and subscripts 3,2 refer to 3-D and 2-D roughnesses respectively.
In particular for hemispherical or semi cylindrical roughnesses of radius a, in a hard boundary,

$$\alpha_{3D} \simeq \frac{7}{16\pi N} \sigma_v^3 k_0^6, \quad \sigma_v = \frac{2N}{3} \pi a^3$$

and

$$\alpha_{2D} \simeq \frac{3}{4N} \sigma_v^3 k_0^5, \quad \sigma_v = \frac{N\pi a^2}{2}$$

respectively.

RESULTS

1. COMPARISONS WITH DATA

Measurements of excess attenuation above various smooth and artificially-roughened boundaries have been made in an anechoic chamber[15].
A smooth boundary consisted of a varnished-wooden board measuring 1.2 m x 1.2 m x 0.02 m (thick). Forty varnished halves of 1 m long wooden dowel rods (0.006 m radius) were used as two dimensional roughnesses and placed at regular spacing on the board between source and receiver. Figure 1(b) shows an example comparison between measured and predicted excess attenuation spectra with source and receiver at 0.145 m height and separated by 1 m. The measured influence of these roughnesses is to change the frequency of the primary ground effect dip from 4 kHz to a little more than 3 kHz and to deepen it from 25 to 32 dB. Figure 1(a) shows a prediction obtained by assuming that the (smooth) varnished board has a small but finite admittance corresponding to a rigid-porous medium with triangular pores[21], porosity 0.1, flow resistivity 500,000 kN s m^{-4}, tortuosity 1, and that the effect of the roughnesses is modelled by equations (6) and (7) (the curve labelled MH). Also shown is a prediction obtained from equations (2) and (8) using an impedance for the scatterers corresponding to that of a rigid-porous medium with triangular pores[18], porosity 0.1, flow resistivity 750 kN s m^{-4} tortuosity 1 (the curve labelled MT). The agreement between prediction (MT) and measurement is good.

2. NUMERICAL FAR-FIELD ESTIMATES

Figure 2 shows the estimated ratio of rough to smooth fields as a function of range in the presence of a weak bilinear sound velocity gradient of 0.005 ms^{-1} m^{-1} at 500 Hz. Close packed 3-D or 2-D roughnesses of 0.025 m radius are assumed and attenuation due to incoherent scatter is included. Increases of level deep in the shadow zone by more than 20 dB are predicted as a consequence of close packed 3-D ground roughnesses. Incoherent scatter reduces the effect of 2-D roughnesses in comparison.
Figures 3 and 4 show predicted roughness effects in the refractive shadow zone above a finite impedance surface. Clearly the influence of a given (3-D) roughness is much reduced if the ground has a small but finite admittance.

CONCLUSIONS

Measurements show that surface roughness has a significant influence on ground effect (homogeneous atmosphere). Predictions of propagation over a rough finite impedance boundary using two alternative models (MH and MT) for the effective surface admittance have been validated by data.
Tolstoy's theory for far-field propagation into the shadow zone caused by a weak velocity gradient in the atmosphere predicts substantial penetration by the rough surface boundary wave over a rough hard ground surface even when attenuation due to incoherent scatter is included. For a given mean roughness height and close-packing, 3-D roughnesses result in greater penetration than 2-D roughnesses.
Modifications of Tolstoy's theory to account for finite impedance predict that in the far-field and high frequency limits the shadow zone penetration is much less when the ground impedance is finite.

ACKNOWLEDGEMENTS

This work was supported by EPSRC Grant No. GR/J 24052. The measurements reported in this paper were made by Shahram Taherzadeh.

REFERENCES

1. K. Attenborough Applied Acoustics **24** 289-319 (1988).
2. I. Tolstoy J. Acoust.Soc.Am. **75** (1) 1-22 (1984).
3. I. Tolstoy **72** (3) 960-972 (1982).
4. I. Tolstoy J.Acoust.Soc.Am. **78** (5) 1727-1734 (1985).
5. H. Medwin, J. Baillie, J. Bremhorst, B.J. Savage and I. Tolstoy J.Acoust.Soc.Am. **66**(4) 1131-1134 (1979).
6. H.. Medwin, G.L. D'Spain, E. Childs and S.J. Hollis J.Acoust.Soc.Am. **76** (6) 1774-1791 (1984).
7. H. Medwin and G.L. D'Spain J.Acoust.Soc.Am. **79** (3) 657-665 (1986).
8. M.A. Biot J.Acoust.Soc.Am. **29** 1192-1200 (1957).
9. V.F. Twersky J.Acoust.Soc.Am. **29** 209-225 (1957).
10. I. Tolstoy J.Acoust.Soc.Am. **69** 1290-1298 (1981).
11. H. Medwin and J.C. Novarini J.Acoust.Soc.Am. **76** (6) 1791-1797 (1984).
12. M.S. Howe J.Sound Vib. **98** (1) 83-94 (1985).
13. K. Attenborough and S. Taherzadeh J.Acoust.Soc.Am. (to be published).
14. I. Tolstoy J.Acoust.Soc.Am. **77** (2) 482-488 (1985).
15. K. Attenborough, S.I. Hayek and J.M. Lawther J.Acoust.Soc.Am. **68** (5) 1493-1501 (1980).
16. A. Pierce publ. Acoustical Society of America, American Institute of Physics, New York (1991).
18. K. Attenborough Acta Acustica **1** 213-226 (1993).

Effects of semicylindrical roughnesses on excess attenuation over wooden boundary

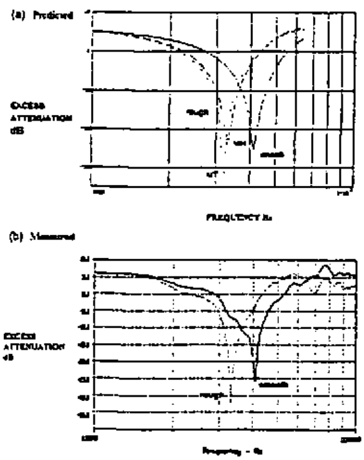

Predictions for source and receiver at 0.145 m height and 1 m separation with wooden base characterised by flow resistivity 500000 kN s m⁻⁴, porosity 0.1, tortuosity 1 and 0.004 mm semicylindrical scatterers characterised by flow resistivity 750 kN s m⁻⁴ porosity 0.1 and tortuosity 1.

Figure 1

Far-field propagation at grazing incidence into the refractive shadow zone over a rough hard boundary

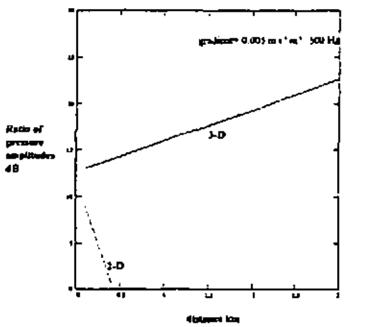

Predicted ratio of pressure in a rough surface boundary wave to the diffracted field in shadow zone caused by weak upward refracting atmosphere (-0.005 m s⁻¹/m) at 500 Hz. Close-packed roughnesses of 0.025 m radius are either hemispherical or cylindrical. Attenuation due to incoherent scatter is included.

Figure 2

Propagation at grazing incidence into the refractive shadow zone over a rough finite impedance boundary at 200 Hz

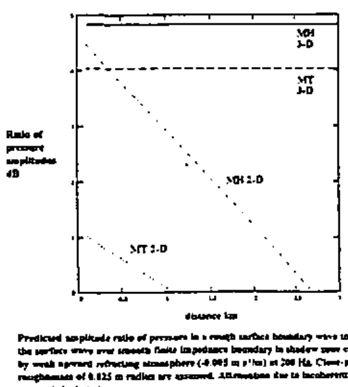

Predicted amplitude ratio of pressure in a rough surface boundary wave to that in the surface wave over smooth finite impedance boundary in shadow zone caused by weak upward refracting atmosphere (-0.005 m s⁻¹/m) at 200 Hz. Close-packed roughnesses of 0.025 m radius are assumed. Attenuation due to incoherent scatter is included.
Finite impedance is modelled by flow resistivity 1000 kPa s m⁻², porosity 0.2, tortuosity 3.

Figure 3

Propagation at grazing incidence into the refractive shadow zone over a rough finite impedance boundary

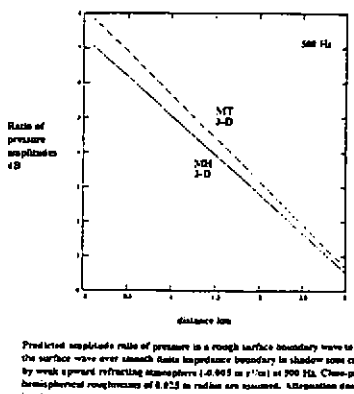

Predicted amplitude ratio of pressure in a rough surface boundary wave to that in the surface wave over smooth finite impedance boundary in shadow zone caused by weak upward refracting atmosphere (-0.005 m s⁻¹/m) at 500 Hz. Close-packed hemispherical roughnesses of 0.025 m radius are assumed. Attenuation due to incoherent scatter is included.
Finite impedance is modelled by flow resistivity 1000 kPa s m⁻², porosity 0.2, tortuosity 3.

Figure 4